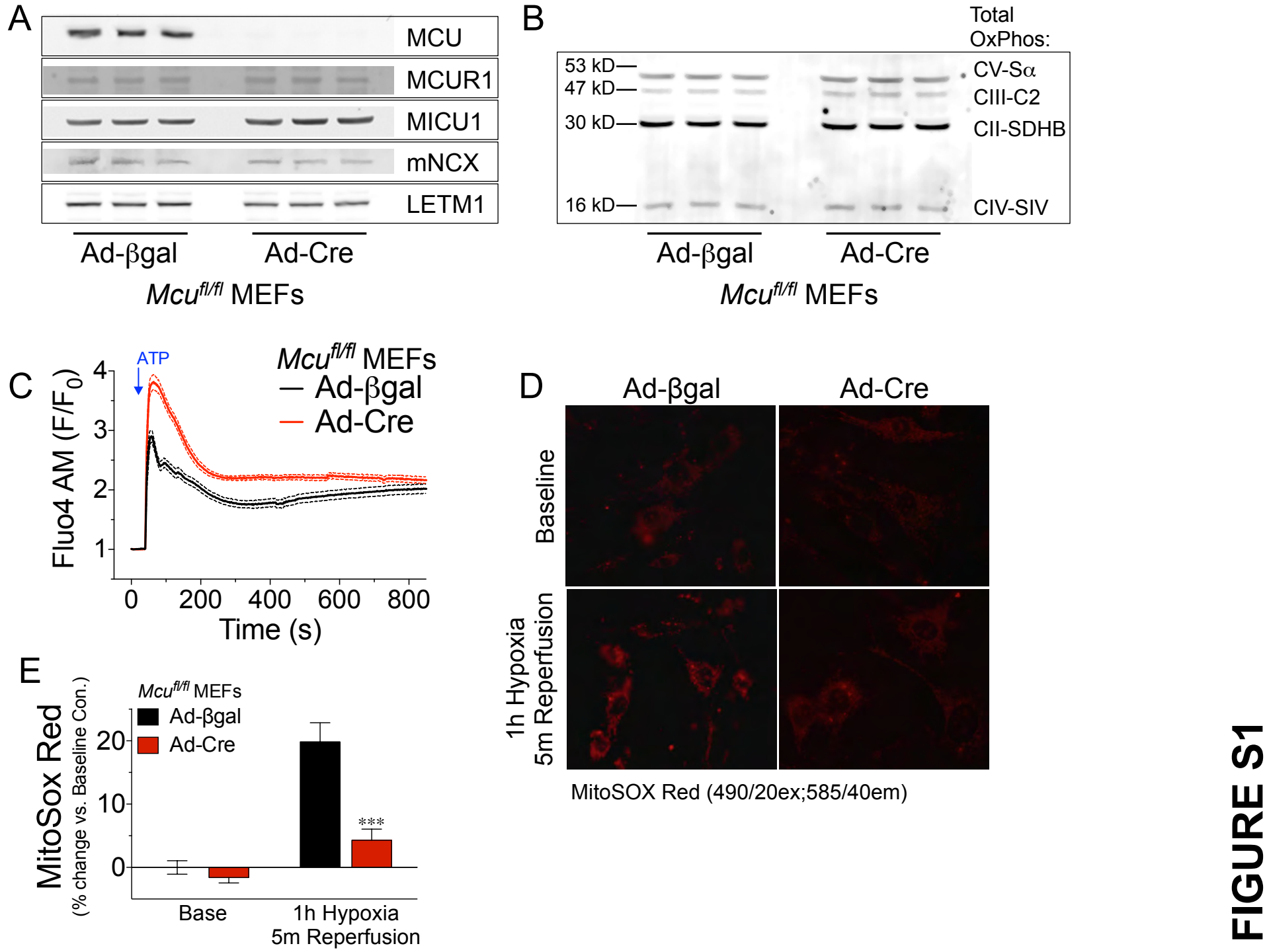
A
MCU
MCUR1
MICU1
mNCX
LETM1
Ad-βgal
Ad-Cre
Mcu fl/fl MEFs
B
Total OxPhos:
53 kD
47 kD
30 kD
16 kD
CV-Sα
CIII-C2
CII-SDHB
CIV-SIV
Ad-βgal
Ad-Cre
Mcu fl/fl MEFs
C
ATP
Mcu fl/fl MEFs
Ad-βgal
Ad-Cre
Fluo4 AM (F/F0)
Time (s)
D
Ad-βgal
Ad-Cre
Baseline
1h Hypoxia
5m Reperfusion
MitoSOX Red (490/20ex;585/40em)
E
MitoSox Red
(% change vs. Baseline Con.)
Mcu fl/fl MEFs
Ad-βgal
Ad-Cre
***
Base
1h Hypoxia
5m Reperfusion

FIGURE S1

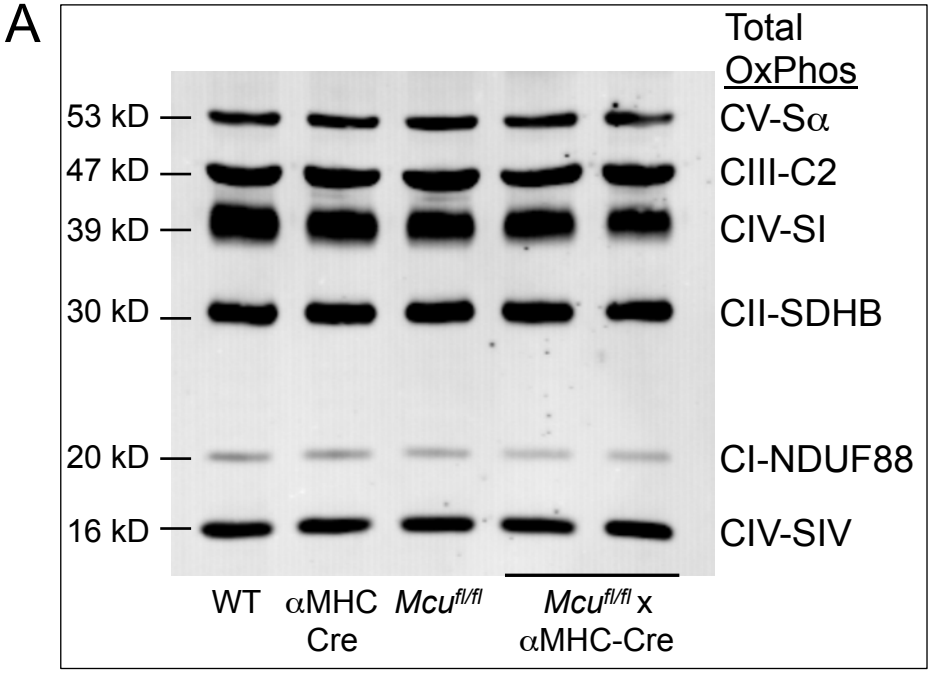
A
Total
OxPhos
53 kD
47 kD
39 kD
30 kD
20 kD
16 kD
CV-Sα
CIII-C2
CIV-SI
CII-SDHB
CI-NDUF88
CIV-SIV
WT
αMHC Cre
Mcu fl/fl
Mcu fl/fl x αMHC-Cre

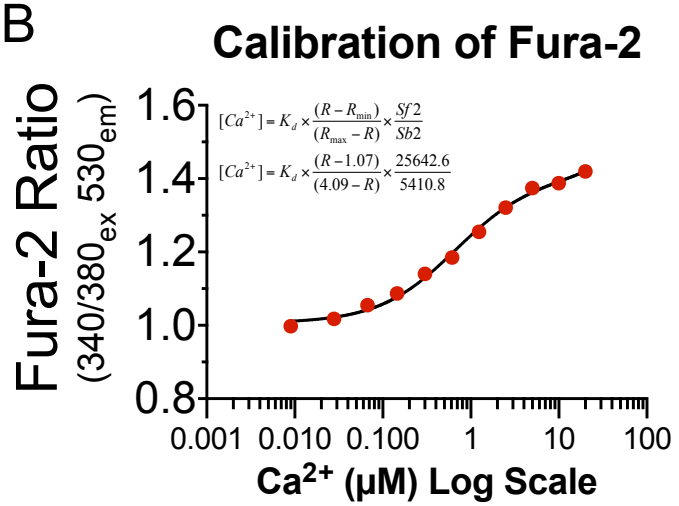
B
Calibration of Fura-2
Fura-2 Ratio (340/380ex 530em)
1.6
1.4
1.2
1.0
0.8
0.001
0.010
0.100
1
10
100
Ca2+ (μM) Log Scale

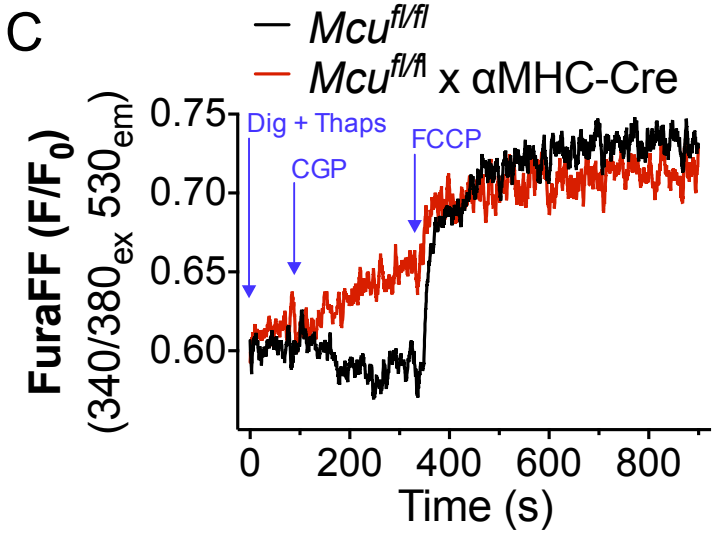
C
Mcu fl/fl
Mcu fl/fl x αMHC-Cre
FuraFF (F/F0) (340/380ex 530em)
0.75
0.70
0.65
0.60
Dig + Thaps
CGP
FCCP
0
200
400
600
800
Time (s)

FIGURE S2

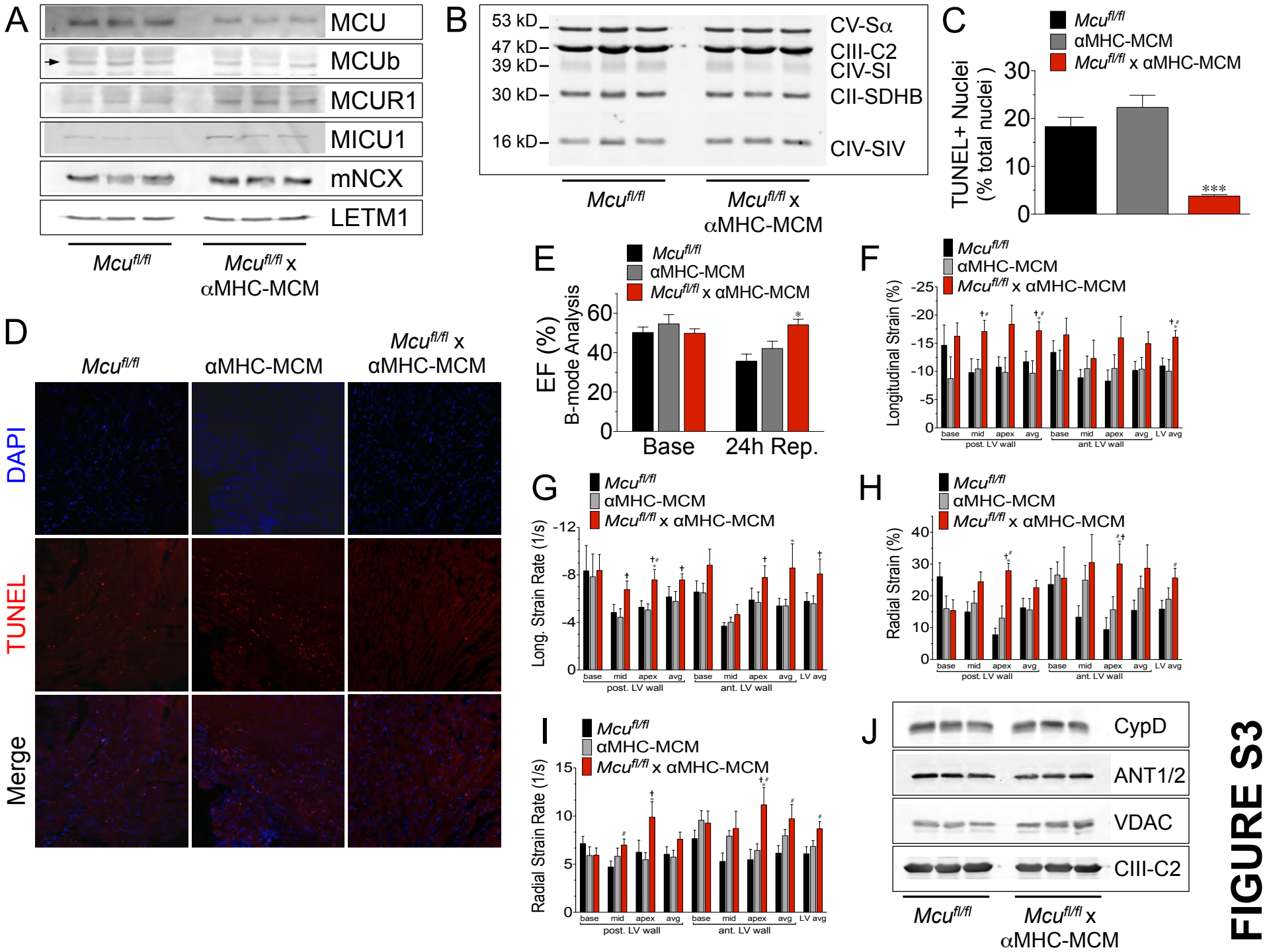
A
MCU
MCUb
MCUR1
MICU1
mNCX
LETM1
Mcu fl/fl
Mcu fl/fl x αMHC-MCM
B
53 kD
47 kD
39 kD
30 kD
16 kD
CV-Sα
CIII-C2
CIV-SI
CII-SDHB
CIV-SIV
Mcu fl/fl
Mcu fl/fl x αMHC-MCM
C
Mcu fl/fl
αMHC-MCM
Mcu fl/fl x αMHC-MCM
TUNEL+ Nuclei (% total nuclei)
***
D
Mcu fl/fl
αMHC-MCM
Mcu fl/fl x αMHC-MCM
DAPI
TUNEL
Merge
E
EF (%) B-mode Analysis
Base
24h Rep.
F
Longitudinal Strain (%)
base mid apex avg base mid apex avg LV avg
post. LV wall
ant. LV wall
G
Long. Strain Rate (1/s)
H
Radial Strain (%)
I
Radial Strain Rate (1/s)
J
CypD
ANT1/2
VDAC
CIII-C2
Mcu fl/fl
Mcu fl/fl x αMHC-MCM

FIGURE S3

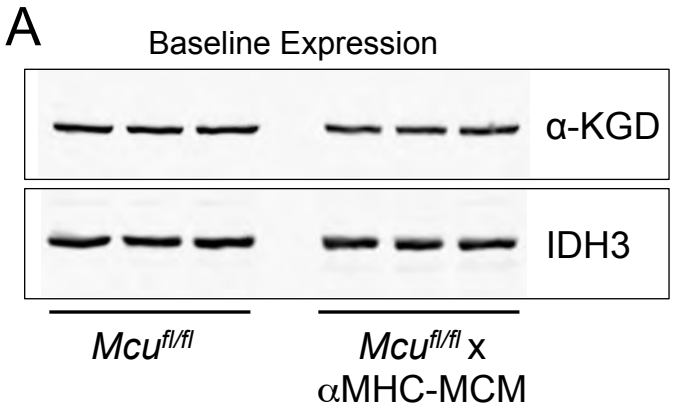
A
Baseline Expression
α-KGD
IDH3
Mcu^fl/fl
Mcu^fl/fl x αMHC-MCM

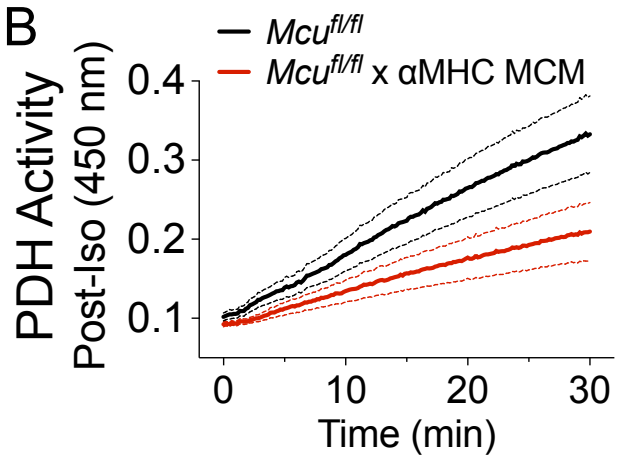
B
Mcu^fl/fl
Mcu^fl/fl x αMHC MCM
PDH Activity
Post-Iso (450 nm)
0.4
0.3
0.2
0.1
0
10
20
30
Time (min)

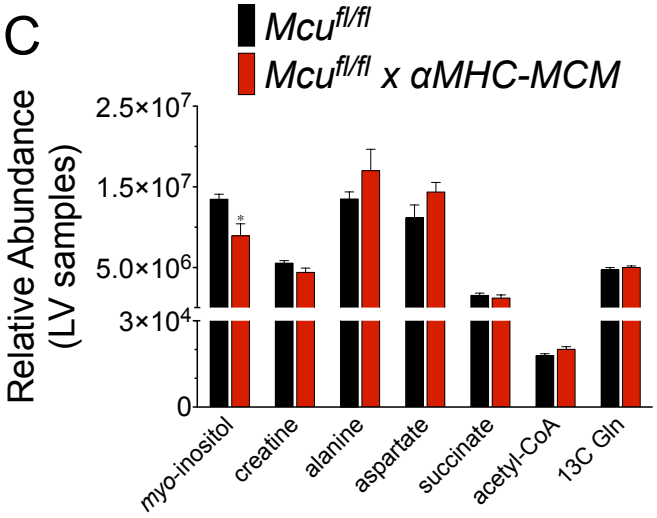
C
Mcu^fl/fl
Mcu^fl/fl x αMHC-MCM
Relative Abundance
(LV samples)
2.5×10^7
1.5×10^7
5.0×10^6
3×10^4
0
*
myo-inositol
creatine
alanine
aspartate
succinate
acetyl-CoA
13C Gln

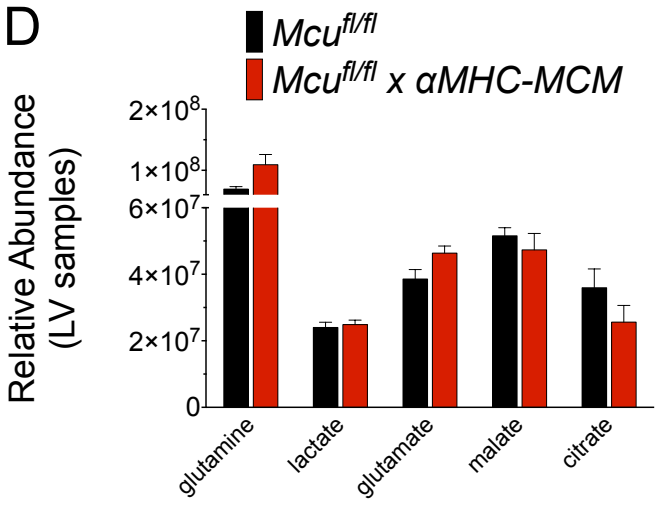
D
Mcu^fl/fl
Mcu^fl/fl x αMHC-MCM
Relative Abundance
(LV samples)
2×10^8
1×10^8
6×10^7
4×10^7
2×10^7
0
glutamine
lactate
glutamate
malate
citrate

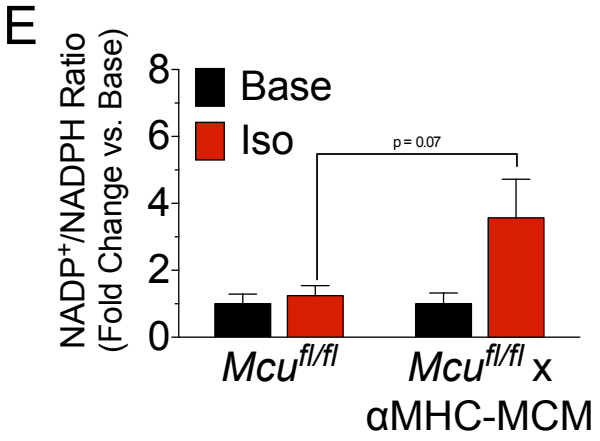
E
NADP+/NADPH Ratio
(Fold Change vs. Base)
Base
Iso
p = 0.07
8
6
4
2
0
Mcu^fl/fl
Mcu^fl/fl x
αMHC-MCM

FIGURE S4

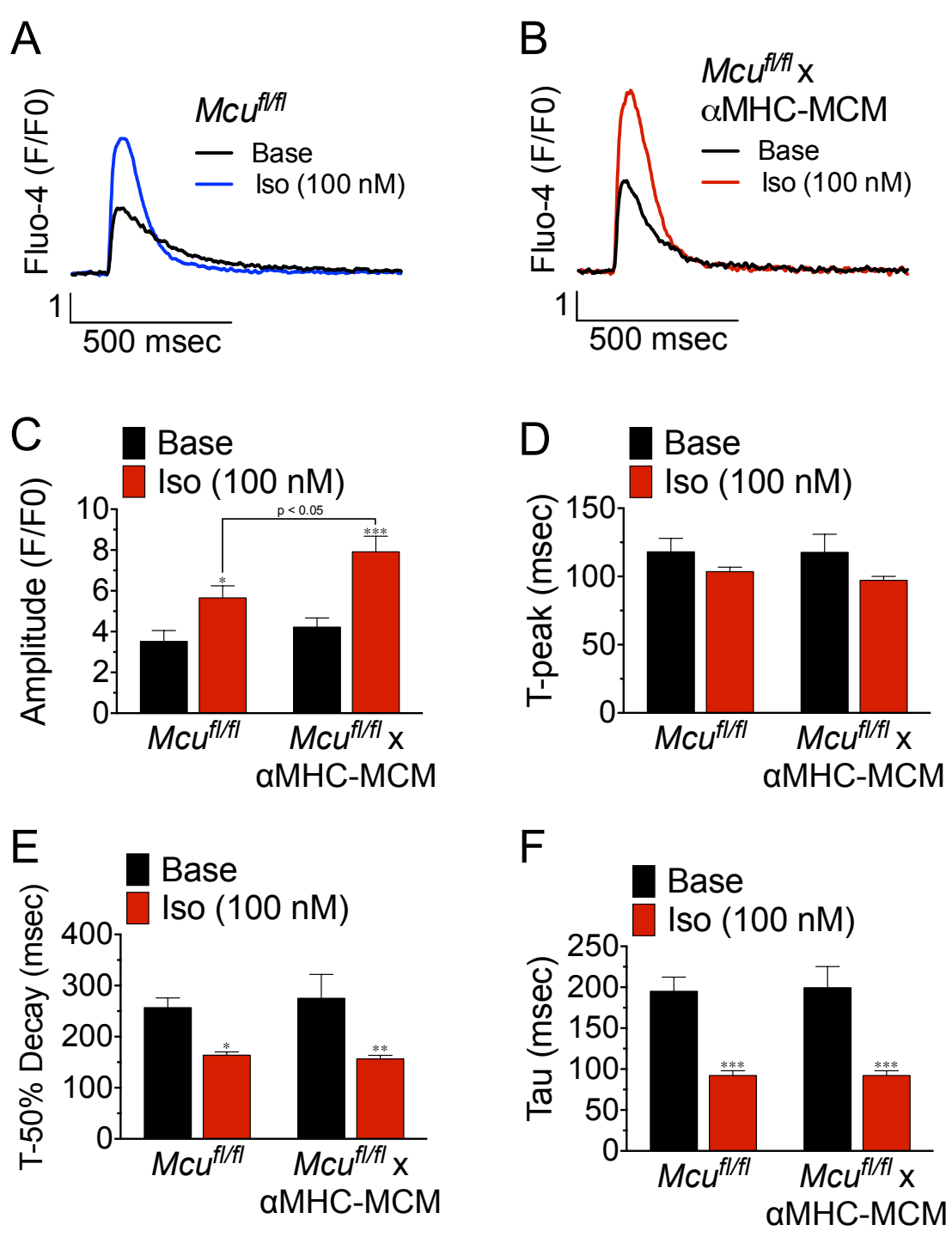
A
Mcu fl/fl
Base
Iso (100 nM)
Fluo-4 (F/F0)
1
500 msec
B
Mcu fl/fl x
αMHC-MCM
Base
Iso (100 nM)
Fluo-4 (F/F0)
1
500 msec
C
Base
Iso (100 nM)
p < 0.05
Amplitude (F/F0)
Mcu fl/fl
Mcu fl/fl x
αMHC-MCM
D
Base
Iso (100 nM)
T-peak (msec)
Mcu fl/fl
Mcu fl/fl x
αMHC-MCM
E
Base
Iso (100 nM)
T-50% Decay (msec)
Mcu fl/fl
Mcu fl/fl x
αMHC-MCM
F
Base
Iso (100 nM)
Tau (msec)
Mcu fl/fl
Mcu fl/fl x
αMHC-MCM

FIGURE S5

SUPPLEMENTAL FIGURE LEGENDS

Figure S1 – *related to Fig 1*. *Mcu* KO MEF $_{m}Ca^{2+}$ exchanger protein expression, $_{i}Ca^{2+}$ transients, and hypoxia/reoxygenation mediated mitochondrial superoxide production. MEFs were treated with Ad-Cre or Ad-βgal 6d prior to all experiments. **A**) Immunoblots for candidate MCU complex genes: MCU, MCUR1, and MICU1 and $_{mito}Ca^{2+}$ exchange proteins: mNCX and LETM1. **B**) Immunoblot of OxPhos complexes: Complex II succinate dehydrogenase subunit B (CII-SDHB) ~ 30kD, Complex III subunit Core 2 (CIII-C2) ~ 47kD, Complex IV subunit IV (CIV-SIV) ~ 16kD, ATP synthase subunit α (CV-Sα) ~ 53kD. **C**) Cytosolic Ca^{2+} transient after stimulation with 1-mM ATP using the Ca^{2+} sensor, Fluo4-AM. **D-E**) MEFs were loaded with MitoSOX Red (490/20ex; 585/40em) to evaluate mitochondrial superoxide production at baseline and after 1h hypoxia and 5min reperfusion. Mitochondrial superoxide production expressed as percent change vs. baseline of Ad-βgal. *(***p<0.001 vs. $Mcu^{fl/fl}$* Ad-βgal)

Figure S2 – *related to Fig 2*. Protein expression of ETC components, calibration of Fura-Ca^{2+} reporter, and $_{m}Ca^{2+}$ content recordings without pharmacologic MCU inhibition. **A**) Adult cardiomyocytes isolated from: wild-type (WT), αMHC-Cre (Cre), *$Mcu^{fl/fl}$, and $Mcu^{fl/fl}$* x Cre mice. Samples were lysed and subjected to western blot analysis for various OxPhos components including: Complex I subunit NDUFB8 (CI-NDUF88) ~ 20kD, Complex II succinate dehydrogenase subunit B (CII-SDHB) ~ 30kD, Complex III subunit Core 2 (CIII-C2) ~ 47kD, Complex IV subunit I (CIV-SI) ~ 39kD, Complex IV subunit IV (CIV-SIV) ~ 16kD, ATP synthase subunit α (CV-Sα) ~ 53kD. **B**) Fura-2 was calibrated by the generation of a standard curve of Ca^{2+} (0.010 - 20 μM) in experimental intracellular buffer to quantify actual Ca^{2+} content as shown in Figure 2C. Fura-2 fluorescence ratio was converted to [Ca^{2+}] by the following equation: [Ca^{2+}] = Kd * (R-Rmin) / (Rmax - R) * Sf2 / Sb2 (Rmin = ratio in 0-Ca^{2+}, Rmax = ratio at saturation, Sf2 = 380/510 reading in 0-Ca^{2+}, Sb2 = 380/510 reading with Ca^{2+} saturation). **C**) ACMs were isolated and loaded with the Ca^{2+} sensor Fura-FF. The sarcolemma was permeabilized with digitonin in the presence of thapsigargin (SERCA inhibitor), CGP-37157 was added at 150s (mNCX inhibitor) and Ca^{2+} levels were recorded and upon reaching a stable baseline, free-Ca^{2+} was released from the mitochondrial matrix with FCCP. It was observed that any Ca^{2+} liberated during our experimental procedure, such as SERCA inhibition, was immediately taken up by WT mitochondria (black trace) in a MCU-dependent fashion.

Figure S3 – *related to Fig 3*. Western blot assessment of MCU components, $_{m}Ca^{2+}$ exchangers, and ETC complexes following tamoxifen-mediated *Mcu* deletion, and TUNEL Staining 24h Post-I/R. *$Mcu^{fl/fl}$* and *$Mcu^{fl/fl}$* x αMHC-Mer-Cre-Mer (αMHC-MCM) mice were treated with tamoxifen (40 mg/kg/day) for 5d to delete *Mcu* and 1wk later examined for changes in protein expression. **A**) Immunoblots for candidate MCU complex genes: MCU, MCUb, MCUR1, MICU1 and $_{m}Ca^{2+}$ exchangers' mNCX and LETM1. **B**) Immunoblot of OxPhos complexes: Complex II succinate dehydrogenase subunit B (CII-SDHB) ~ 30kD, Complex III subunit Core 2 (CIII-C2) ~ 47kD, Complex IV subunit I (CIV-SI) ~ 39kD, Complex IV subunit IV (CIV-SIV) ~ 16kD, ATP synthase subunit α (CV-Sα) ~ 53kD. **C-D**) TUNEL Staining of paraffin-embedded heart sections 24h post-I/R, co-stained with DAPI and quantified as percent TUNEL positive nuclei vs. total nuclei in the infarct border zone. **E-I**) B-mode speckle-tracking analysis of LV function. **E**) Percent ejection fraction (EF%). **F**) Longitudinal Stain (%). **G**) Longitudinal strain Rate (1/s). **H**) Radial strain (%). **I**) Radial Stain rate (1/s). **J**) Immunoblots of cyclophilin-D (CypD), adenine nucleotide translocator (ANT1/2), voltage-dependent anion channel (VDAC) and loading control complex-III C2 from *$Mcu^{fl/fl}$* and *$Mcu^{fl/fl}$* x αMHC-MCM ACMs. *(*p<0.05 vs.*

*$Mcu^{fl/fl}$ and αMHC MCM, ***p<0.001 vs. $Mcu^{fl/fl}$ and αMHC MCM #p<0.05 vs. $Mcu^{fl/fl}$, †p<0.05 vs. αMHC MCM)*

Figure S4 – *related to Fig 4*. Quantification of LV metabolites, baseline expression of mitochondrial dehydrogenases, PDH activity rates, and $NADP^+$/NADPH ratio. A) Immunoblot of baseline expression of α-ketogluterate dehydrogenase (αKGD) and isocitrate dehydrogenase (IDH3). **B**) Traces of PDH activity from heart tissue post-isoproterenol administration (OD read at 450 nm). Dashed lines represent SEM. **C-D**) Mice 10wk of age were injected i.p. with 40mg/kg/d tamoxifien for 5d. 2wks later hearts were removed and snap-frozen in liquid nitrogen for LC-MS/MS metabolomic analysis. Relative abundance of various TCA metabolite levels. *(n=3 for all groups, *p<0.05 vs. $Mcu^{fl/fl}$).* **E**) $NADP^+$/NADPH ratio at baseline and post-isoproterenol represented as fold-change vs. baseline.

Figure S5 – *related to Fig 5*. Cytosolic Ca^{2+} transients in *Mcu* cKO isolated adult cardiomyocytes at baseline and following isoproterenol administration. ACMs were loaded with the cytosolic Ca^{2+} sensor, Fluo-4 AM and $_iCa^{2+}$ was examined during pacing at 0.5 Hz. **A**-**B**) Representative traces of $_iCa^{2+}$ transients at baseline and during Iso. **C**) Amplitude calculated as (F/F0). **D**) Time-to-peak of $_iCa^{2+}$ transients. **E**) Time-to-50% decay. **F**) Tau (rate of decay) of $_iCa^{2+}$ transients. *(*p<0.05 vs. $Mcu^{fl/fl}$, **p<0.01 vs. $Mcu^{fl/fl}$, ***p<0.001 vs. $Mcu^{fl/fl}$)*

Table S1 – *related to Fig 3*.

	Strain	n	IVS;d (mm)	IVS;s (mm)	LVID;d (mm)	LVID;s (mm)	LVPW;d (mm)	LVPW;s (mm)	EF (%)	FS (%)	LV Vol;d (µl)	LV Vol;s (µl)
Base	*Mcu*$^{fl/fl}$	9	0.88 ± 0.03	1.19 ± 0.03	3.34 ± 0.18	2.25 ± 0.16	0.99 ± 0.07	1.30 ± 0.07	62.3 ± 2.0	33.1 ± 2.1	47.3 ± 5.68	18.6 ± 3.14
	αMHC-MCM	8	0.95 ± 0.03	1.22 ± 0.05	3.33 ± 0.24	2.24 ± 0.20	0.94 ± 0.04	1.28 ± 0.07	61.9 ± 2.2	32.4 ± 1.4	47.5 ± 8.43	19.2 ± 4.28
	Mcu$^{fl/fl}$ x αMHC-MCM	8	0.89 ± 0.02	1.17 ± 0.05	3.82 ± 0.13	2.66 ± 0.08	0.83 ± 0.06	1.20 ± 0.08	57.8 ± 2.2	30.1 ± 1.5	63.5 ± 5.02	26.5 ± 2.03
24h Post-IR	*Mcu*$^{fl/fl}$	8	0.94 ± 0.03	1.14 ± 0.05	3.92 ± 0.17	3.18 ± 0.22	1.13 ± 0.16	1.38 ± 0.18	39.6 ± 5.6	19.2 ± 2.9	67.9 ± 6.68	42.2 ± 6.94
	αMHC-MCM	8	0.92 ± 0.04	1.19 ± 0.07	3.52 ± 0.17	2.80 ± 0.18	0.98 ± 0.06	1.14 ± 0.05	43.2 ± 3.7	20.9 ± 2.0	53.1 ± 6.19	31.0 ± 4.90
	Mcu$^{fl/fl}$ x αMHC-MCM	7	1.02 ± 0.13	1.39± 0.18	3.43 ± 0.43	2.35 ± 0.30*	0.86 ± 0.10	1.15 ± 0.13	60.7 ± 7.7**	32.0 ± 4.3**	49.0 ± 6.43	20.0 ± 3.24*

Table S1 – *related to Fig 3*. Echocardiographic results of left-ventricular (LV) function at baseline (base) and 24h post-IR. All values were collected from M-mode analyses to measure intraventricular septum thickness (IVS), left-ventricular interior dimensions (LVID), Left-ventricular posterior wall thickness (LVPW), left-ventricular volume (LV Vol) during diastole (d) and systole (s), percent ejection fraction (EF), and percent fractional shortening (FS). *(*p<0.05 vs. Mcu$^{fl/fl}$ and αMHC MCM)*

SUPPLEMENTAL EXPERIMENTAL PROCEDURES

Generation of Mcu conditional knockout mice*. Mcu* conditional knockout mice were generated in collaboration with the HHMI Gene Targeting & Transgenic Facility at the Janelia Research Campus. Insertion of a targeting construct containing loxP sites flanking exons 5 - 6 of the *Mcu* gene (ch10: 58930544-58911529) was performed in mouse ES cells. Three independent mutant ES cell lines were confirmed and subjected to morula aggregation and subsequent embryos transplanted into pseudo-pregnant females. Two of the three mutant ES cell lines produced germline mutant mice, which were crossed with ROSA26-FLPe knock-in mice for removal of the FRT-flanked neomycin cassette. Resultant $Mcu^{fl/fl}$ mice were crossed with cardiac specific-Cre transgenic mice, αMHC-Cre and αMHC-MCM, to generate cardiomyocyte-specific *Mcu* knockouts. B6.CMV-Cre transgenic mice (Jackson Laboratory, Stock # 006054) were used to attempt germline deletion. For temporal deletion of *Mcu* using the αMHC-MCM model, $Mcu^{fl/fl}$, αMHC-MCM, and $Mcu^{fl/fl}$ x αMHC-MCM were injected i.p. with 40 mg/kg/day of tamoxifien for 5 consecutive days. For all experiments mice were 10-14 wks of age. All mutant lines were maintained on the C57/BL6 background and all experiments involving animals were approved by Temple University's IACUC and followed AAALAC guidelines.

Western blot analysis*.* All tissue samples were lysed by homogenization in RIPA buffer. Samples were run by electrophoresis on 10% and 12% polyacrylamide Tris-glycine SDS gels. The following antibodies were used in the study: MCU, (1:1,000), Sigma-Aldrich; MCUb (1:1,000, Abgent; CCDC90A (MCUR1) (1:1,000), Abcam); MICU1 (1:500), Custom generation by Yenzyme, courtesy of the Madesh Lab; VDAC (1:2,500), Abcam; ANT (1:1,000), Santa Cruz Biotech; Cyclophilin D (1:5,000), Abcam; NCLX (mNCX) (1:1000), Santa Cruz N-12; LETM1 (1:1,000), Proteintech; ETC respiratory chain complexes (1:1,000), OxPhos Cocktail, Abcam; PDH subunits (1:1,000), Abcam; p-PDH^{S293} (1:1,000), Abcam; αKGD (1:250), Santa Cruz; IDH3 (1:500), Abcam; and Licor IR secondary antibodies (1:12,000). All images were acquired using a Licor Odyssey system. All procedures were carried out as previously reported (Elrod et al., 2010).

Isolation of adult mouse cardiomyocytes*.* Myocytes were isolated from ventricular tissue of mice as previously reported (Zhou et al., 2000). Briefly, mice were injected with heparin (1,500 U/kg) and anesthetized. Hearts were excised and the aorta was cannulated and perfused with a Ca^{2+}-free bicarbonate buffer (120 mM NaCl, 5.4 KCl mM, 1.2 $MgSO_4$ mM, 1.2 mM NaH_2PO_4, 5.6 mM glucose, 20 mM NaHCO3, 10 mM 2,3-butanedione monoxime (BDM) and 5 mM taurine, gassed with 95% O2–5% CO2) at 37°C and then digested with collagenase B (1 mg/ml, Roche) supplemented with 0.05 mM Ca^{2+} and protease XIV (0.02 mg/ml, Sigma). Heart tissue was then cut into small pieces and aggregated by gentle pipetting to release the myocytes. Ca^{2+} was recovered with 10 min incremental additions (0.125 mM, 0.25 mM, 0.5 mM, 1 mM). Myocytes were then incubated at 37 °C with 5% CO_2. All cells were used within 3h of isolation.

Evaluation of $_mCa^{2+}$ uptake and content*.* To evaluate $_mCa^{2+}$ uptake and content, isolated adult cardiomyocytes were transferred to an intracellular-like medium containing (120-mM KCl, 10-mM NaCl, 1-mM KH_2PO_4, 20-mM HEPES-Tris), 3-μM thapsigargin, 80-μg/ml digitonin, protease inhibitors (Sigma EGTA-Free Cocktail), supplemented with 10-μM succinate and pH to 7.2. All solutions were cleared with Chelex 100 to remove trace Ca^{2+} (Sigma). For $_mCa^{2+}$ content: 150,000 digitonin permeabilized adult cardiomyocytes were treated with 1-μM Ru360 and 10-μM CGP-37157 to inhibit $_mCa^{2+}$ exchange. The myocytes were gently stirred and 1-μM Fura-2

(Invitrogen) was added to monitor extra-mitochondrial Ca^{2+}. Fluorescence signals were monitored in a spectrofluorometer (Delta RAM, Photon Technology Int.) at 340- and 380-nm ex/510-nm em. After acquiring baseline recordings, at 200s, 10-μM FCCP was added to uncouple the $\Delta\psi_m$ and release matrix free-Ca^{2+} (Miller et al., 2014).

To calibrate $_mCa^{2+}$ content, a standard curve of Ca^{2+} binding Fura-2 was generated from serial diluted Ca^{2+} standards (20 - 0.010 μM) in intracellular buffer. The Kd was calculated from the standard curve using Graphpad Prism 6.0 software. The fluorescence intensity was corrected to [Ca^{2+}] by the following equation: [Ca^{2+}] = Kd * (R-Rmin) / (Rmax - R) * Sf2 / Sb2 (Rmin=1.07, Rmax= 4.097, Sf2= 25642.6, Sb2= 5410.77).

To measure $_mCa^{2+}$ uptake capacity, 300,000 adult cardiomyocytes were gently stirred and 1 μM Fura-FF (Invitrogen) was added to monitor extra-mitochondrial Ca^{2+}. At 20s JC-1 (Enzo Life Sciences) was added to monitor $\Delta\psi_m$. Fluorescence signals were monitored at 490-nm excitation (ex)/535-nm emission (em) for the monomer, 570-nm ex/595-nm em for the J-aggregate of JC-1, and 340- and 380-nm ex/510-nm em for Fura-FF. Starting at 450 sec 10 μM Ca^{2+} boluses were added every 60 sec for 9 boluses. At 20s JC-1 was added to monitor Δψ. Fluorescence signals for JC-1 were monitored at 490ex/535 em for the monomer and 570ex/595em for the J-aggregate. Fura was monitored at 340/380ex and 510em. Starting at 450s 10 μM Ca^{2+} boluses were added every 60s. Clearance of extra-mitochondrial Ca^{2+} was representative of $_mCa^{2+}$ uptake. At completion of the experiment the protonophore, FCCP, was added. All experiments were conducted at 37 °C and recorded on a PTI spectrofluorometer. All details are previously reported (Mallilankaraman et al., 2012).

Mitochondria Isolation and Swelling. Hearts were excised from mice and mitochondria were isolated using a published protocol (Frezza et al., 2007). For the swelling assay, mitochondria were diluted in assay buffer containing (125-mM KCl, 20-mM HEPES, 2-mM $MgCl_2$, 2-mM K_2HPO_4 at pH 7.2) and supplemented with 10-mM succinate. Swelling was monitored using a Tecan Infinite M1000 Pro plate reader measuring absorbance at 540 ± 20 nm every 5 sec. A 500-μM $CaCl_2$ pulse was added to induce mitochondrial swelling +/- 2-μM Cyclosporin A (CsA) (i.e. decrease in absorbance) (Elrod et al., 2010).

***Adult mouse cardiomyocyte Ca^{2+} transient recordings*.** Isolated ACMs were loaded with 1-μM Fluo-4 AM (Invitrogen) and placed in a 37 °C heated chamber on an inverted microscope stage. Myocytes were perfused with a physiological Tyrode's buffer (150-mM NaCl, 5.4-mM KCl, 1.2 mM-$MgCl_2$, 10-mM glucose, 2-mM sodium pyruvate, and 5-mM HEPES, pH 7.4) containing 1-mM Ca^{2+}. Cells were paced at 0.5 Hz and Ca^{2+} transients continuously recorded and analyzed using Clampex10 software (Molecular Devices). After 2-3 min of baseline recording, 100-nM Isoproterenol (Sigma-Aldrich) was applied by changing the perfusion solution. After a stable baseline, 20 continuous Ca^{2+} transients were recorded and averaged for analysis. For intracellular Ca^{2+} fluorescence measurements, the F_0 was measured as the average fluorescence of the cell 100 ms prior to stimulation. The maximal Fluo-4 fluorescence (F) was measured for peak amplitude. Time to peak was calculated as the time from the beginning of the contraction to peak amplitude. Time to 50% decay was calculated as the time from the beginning of the contraction to 50% relaxation. Background fluorescence was subtracted from each experiment before measuring the peak intensity as F/F_0. Tau was measured as the decay rate of the Ca^{2+} transient.

Mitoplast patch-clamp analysis of MCU Current. Following mitochondria isolation from ventricular tissue, mitoplasts were prepared for patch-clamping (Kirichok et al., 2004). I_{MCU} was

recorded using a computer controlled Axon200B patch clamp amplifier with a Digidata 1320A acquisition board (pClamp 10.0 software; Axon Instruments). Mitoplasts were bathed in a solution containing (5-mM $CaCl_2$, 0.3-mM inorganic phosphate, 150-mM sodium gluconate, 5.4 mM-KCl, 10 mM-HEPES, pH 7.2). The pipette solution contained (150-mM sodium gluconate, 5 mM-NaCl, 135-mM sucrose, 10-mM HEPES, and 1.5-mM EGTA, pH 7.2). After formation of a giga-ohm seal (pipette resistance 20–35 mega-ohms), mitoplasts were ruptured with a 200-400mV pulse for a 2-6 ms duration. Mitoplast capacitance was measured (2.2–3.8 picofarads). After capacitance compensation, mitoplasts were held at 0 mV, and I_{MCU} was elicited with a voltage ramp (from −160 to +80 mV, 120 mV/s) as previously described in detail (Hoffman et al., 2013; Hoffman et al., 2014; Kirichok et al., 2004). All recordings were conducted at 30 °C.

Metabolic Assays. Metabolomic analyses were carried out by metabolite profiling of ventricular tissue by LC-MS/MS as described in Jain et al (Jain et al., 2012). To measure NAD^+/NADH and $NADP^+$/NADPH ratios hearts were lysed in PBS supplemented with protease and phosphatase inhibitors (Roche) prior to and after administration of isoproterenol. The ratios were evaluated using Promega NAD/NADH and NADP/NADPH Glo assays. Pyruvate dehydrogenase activity was quantified using the MitoSciences PDH activity assay on post-isoproterenol treated heart tissue. Activity was expressed as OD/min/mg of tissue.

To assess NADH production in isolated adult mouse cardiomyocytes, 150,000 adult cardiomyocytes were suspended in Tyrode's buffer (150-mM NaCl, 5.4-mM KCl, 5-mM HEPES, 10-mM glucose, 2-mM $CaCl_2$, 2-mM sodium pyruvate at pH 7.4) and NADH autofluorescence was read at 350ex/460em using a PTI spectrofluorometer. ACMs were gently stirred and 10-μM isoproterenol was added followed by 2-μM rotenone.

A Seahorse Bioscience XF96 extracellular flux analyzer was employed to measure adult cardiomyocyte oxygen consumption rates (OCR). 5,000 cardiomyocytes/well were plated in XF media pH 7.4 supplemented with 25-mM glucose and 1-mM sodium pyruvate. Basal OCR was measured +/- 10-μM isoproterenol then 1.5 μM FCCP was added to record maximal respiration. Detailed methodology is previously reported (Readnower et al., 2012).

Echocardiography. Trans-thoracic echocardiography of the LV was performed and analyzed on a Vevo 2100 imaging system (VisualSonics) as previously reported (Elrod et al., 2007). Mice were anesthetized with 2% isoflurane in 100% oxygen during acquisition. B-mode and M-mode images were collected in long- and short-axis. M-mode axis and B-mode strain analysis were performed using VisualSonics software for both short- and long-axis images.

Invasive hemodynamic measurements. Mice were anesthetized (avertin, 25 mg/kg) and a cutdown was performed and right carotid artery isolated for insertion of a 1.4-F pressure catheter (SPR-671, Millar Instruments) that was advanced into the LV. Right jugular vein catheterization allowed delivery of (0, 0.1, 0.5, 1, 5, 10 ng) of isoproterenol during recording. All data was analyzed using Chart 6.0 software. All details have been previously reported (Elrod et al., 2007).

Myocardial IR-Injury. LCA ligation and reperfusion was performed as previously described in Gao et al. (Gao et al., 2010). Briefly, mice were anesthetized with isoflurane and the heart exposed via a left thoracotomy at the fifth intercostal space. A slipknot was tied around the left coronary artery (LCA) to enable ligation. The heart was returned to the chest cavity and the wound was sutured revealing the slipknot. After 40m ischemia, the slipknot was released and the ischemic area was allowed to reperfuse for 24h hours. To assess infarct size, after re-ligation of the LCA, hearts were injected with 3% Evan's Blue to delineate the area not-at-risk and 1mM heart sections were cut using a McIlwain Tissue Chopper. Heart sections were

incubated with 1% triphenyl tetrazolium chloride (TTC) for 5 min at 37 °C to demarcate viable tissue. Each slice was weighed and Image-J was used to quantify infarct area as previously reported (Elrod et al., 2007). Serum was isolated from mice 24h post-IR to measure cardiac troponin I (cTnI) using the Life Diagnostics, Inc. ELISA kit. Cell death was evaluated in the infarct border zone by TUNEL staining using the Roche In Situ Cell Death detection kit, TMR red. Imaged were 4-5 images were taken per slide at 25x objected (TUNEL, 575/35ex and 632/60em; DAPI 360/40ex and 455/50em) and quantified by the percent of TUNEL positive nuclei verses DAPI positive nuclei.

MEF Isolation. Embryos were isolated from pregnant females at E13.5. The embryos were then decapitated and all the red organs removed. Next, tissue was minced up and digested in 0.25% trypsin supplemented with DNase for 10 min at 37°C. Digested tissue was then gently agitated by repeated pipetting to dissociate cells. Cells were then centrifuged at 1000 g for 5 min and the trypsin removed. The cell pellet was suspended in Dulbecco's Modified Eagle's Medium (DMEM) supplemented with 10% fetal bovine serum, non-essential amino acids, and penicillin/streptomycin in a 10 cm plate. Cells were then cultured and treated with Ad-Cre or Ad-βgal for 24h. 6d post-adenovirus treatment cells were used for experiments.

$_{i}Ca^{2+}$ and $_{m}Ca^{2+}$ flux in MEFs. MEFs were infected with AAV-mitycam to measure $_{m}Ca^{2+}$ exchange or loaded with the cytosolic Ca^{2+} indicator, 5-μM Fluo4-AM. Cells were imaged in Tyrode's buffer (150-mM NaCl, 5.4-mM KCl, 5-mM HEPES, 10-mM glucose, 2-mM $CaCl_2$, 2-mM sodium pyruvate at pH 7.4) on a Zeiss 510 confocal microscope using the 488 nm laser. Ca^{2+} flux was assessed in real-time, collecting data every 3s and analyzed on Zen software. $_{m}Ca^{2+}$ uptake capacity in non-excitable cells was evaluated similar to the detailed method provided above and as previously described (Mallilankaraman et al., 2012).

InVitro Hypoxia/Reoxygenation. MEFs were plated onto 35mm glass plates and after culturing for 24h, loaded with 5 μM MitoSOX Red (Invitrogen). Cells were placed in ischemic medium (137-mM NaCl, 12-mM KCl, 4-mM HEPES, 0.49-mM $MgCl_2$, 0.9-mM CaCl2, 10-mM 2-deoxyglucose, 20-mM sodium lactate, 1-mM sodium dithionite at pH 6.5) for 1h and then reperfused in Tyrode's buffer and imaged 5min later (Punn et al., 2000). Cells were imaged (490/20ex; 585/40em) at baseline and 5m following reperfusion to evaluate mitochondrial superoxide production.

Statistics. All results are presented as mean and +/- SEM. Statistical analysis was performed using Prism 6.0 (Graph Pad Software). Where appropriate column analyses were performed using an unpaired, 2-tailed t-test (for 2 groups) or one-way ANOVA with Bonferroni correction (for groups of 3 or more). For grouped analyses either multiple unpaired t-test with correction for multiple comparisons using the Holm-Sidak method or where appropriate 2-way ANOVA with Tukey post-hoc analysis was performed. P values less than 0.05 were considered significant.

SUPPLEMENTAL REFERENCES

Elrod, J.W., Calvert, J.W., Morrison, J., Doeller, J.E., Kraus, D.W., Tao, L., Jiao, X., Scalia, R., Kiss, L., Szabo, C., et al. (2007). Hydrogen sulfide attenuates myocardial ischemia-reperfusion injury by preservation of mitochondrial function. Proceedings of the National Academy of Sciences of the United States of America *104*, 15560-15565.

Elrod, J.W., Wong, R., Mishra, S., Vagnozzi, R.J., Sakthievel, B., Goonasekera, S.A., Karch, J., Gabel, S., Farber, J., Force, T., et al. (2010). Cyclophilin D controls mitochondrial pore-dependent Ca(2+) exchange, metabolic flexibility, and propensity for heart failure in mice. J Clin Invest *120*, 3680-3687.

Frezza, C., Cipolat, S., and Scorrano, L. (2007). Organelle isolation: functional mitochondria from mouse liver, muscle and cultured fibroblasts. Nature protocols *2*, 287-295.

Gao, E., Lei, Y.H., Shang, X., Huang, Z.M., Zuo, L., Boucher, M., Fan, Q., Chuprun, J.K., Ma, X.L., and Koch, W.J. (2010). A novel and efficient model of coronary artery ligation and myocardial infarction in the mouse. Circulation research *107*, 1445-1453.

Hoffman, N.E., Chandramoorthy, H.C., Shamugapriya, S., Zhang, X., Rajan, S., Mallilankaraman, K., Gandhirajan, R.K., Vagnozzi, R.J., Ferrer, L.M., Sreekrishnanilayam, K., et al. (2013). MICU1 motifs define mitochondrial calcium uniporter binding and activity. Cell reports *5*, 1576-1588.

Hoffman, N.E., Chandramoorthy, H.C., Shanmughapriya, S., Zhang, X.Q., Vallem, S., Doonan, P.J., Malliankaraman, K., Guo, S., Rajan, S., Elrod, J.W., et al. (2014). SLC25A23 augments mitochondrial Ca(2)(+) uptake, interacts with MCU, and induces oxidative stress-mediated cell death. Molecular biology of the cell *25*, 936-947.

Jain, M., Nilsson, R., Sharma, S., Madhusudhan, N., Kitami, T., Souza, A.L., Kafri, R., Kirschner, M.W., Clish, C.B., and Mootha, V.K. (2012). Metabolite profiling identifies a key role for glycine in rapid cancer cell proliferation. Science (New York, N.Y *336*, 1040-1044.

Kirichok, Y., Krapivinsky, G., and Clapham, D.E. (2004). The mitochondrial calcium uniporter is a highly selective ion channel. Nature *427*, 360-364.

Mallilankaraman, K., Cardenas, C., Doonan, P.J., Chandramoorthy, H.C., Irrinki, K.M., Golenar, T., Csordas, G., Madireddi, P., Yang, J., Muller, M., et al. (2012). MCUR1 is an essential component of mitochondrial Ca(2+) uptake that regulates cellular metabolism. Nature cell biology *15*, 123.

Miller, B.A., Hoffman, N.E., Merali, S., Zhang, X.Q., Wang, J., Rajan, S., Shanmughapriya, S., Gao, E., Barrero, C.A., Mallilankaraman, K., et al. (2014). TRPM2 channels protect against cardiac ischemia-reperfusion injury: role of mitochondria. The Journal of biological chemistry *289*, 7615-7629.

Punn, A., Mockridge, J.W., Farooqui, S., Marber, M.S., and Heads, R.J. (2000). Sustained activation of p42/p44 mitogen-activated protein kinase during recovery from simulated ischaemia mediates adaptive cytoprotection in cardiomyocytes. The Biochemical journal *350 Pt 3*, 891-899.

Readnower, R.D., Brainard, R.E., Hill, B.G., and Jones, S.P. (2012). Standardized bioenergetic profiling of adult mouse cardiomyocytes. Physiological genomics *44*, 1208-1213.